

Filamin A mutations cause periventricular heterotopia with Ehlers-Danlos syndrome

V.L. Sheen, MD, PhD*; A. Jansen, MD*; M.H. Chen, MD; E. Parrini, PhD; T. Morgan, MSc; R. Ravenscroft, BA; V. Ganesh, BS; T. Underwood, FRACP; J. Wiley, MD; R. Leventer, FRACP; R.R. Vaid, MD, PhD; D.E. Ruiz, MD; G.M. Hutchins, MD; J. Menasha, MD; J. Willner, MD; Y. Geng, MD; K.W. Gripp, MD; L. Nicholson, MS, MC; E. Berry-Kravis, MD; A. Bodell, MS, CGC; K. Apse, ScM; R.S. Hill, PhD; F. Dubeau, MD; F. Andermann, MD; J. Barkovich, MD; E. Andermann, MD; Y.Y. Shugart, PhD; P. Thomas, MD; M. Viri, MD; P. Veggiotti, MD; S. Robertson, FRACP, Dphil; R. Guerrini, MD; and C.A. Walsh, MD, PhD

Abstract—Objective: To define the clinical, radiologic, and genetic features of periventricular heterotopia (PH) with Ehlers-Danlos syndrome (EDS). **Methods:** Exonic sequencing and single stranded conformational polymorphism (SSCP) analysis was performed on affected individuals. Linkage analysis using microsatellite markers on the X-chromosome was performed on a single pedigree. Western blotting evaluated for loss of filamin A (FLNA) protein and Southern blotting assessed for any potential chromosome rearrangement in this region. **Results:** The authors report two familial cases and nine additional sporadic cases of the EDS-variant form of PH, which is characterized by nodular brain heterotopia, joint hypermobility, and development of aortic dilatation in early adulthood. MRI typically demonstrated bilateral nodular PH, indistinguishable from PH due to *FLNA* mutations. Exonic sequencing or SSCP analyses of *FLNA* revealed a 2762 delG single base pair deletion in one affected female. Another affected female harbored a C116 single point mutation, resulting in an A39G change. A third affected female had a 4147 delG single base pair deletion. One pedigree with no detectable exonic mutation demonstrated positive linkage to the *FLNA* locus Xq28, an affected individual in this family also had no detectable FLNA protein, but no chromosomal rearrangement was detected. **Conclusion:** These results suggest that the Ehlers-Danlos variant of periventricular heterotopia (PH), in part, represents an overlapping syndrome with X-linked dominant PH due to *filamin A* mutations.

NEUROLOGY 2005;64:254–262

Periventricular heterotopia (PH) comprises a group of neuronal migration disorders of increasing clinical and genetic diversity. Inheritance may be X-linked dominant (classic bilateral periventricular nodular heterotopia with mutations in the filamin A [*FLNA*] gene)^{1–3} or autosomal recessive (PH and microcephaly with mutations in the *ARFGEF2* gene),^{4,5} although there likely exists an autosomal dominant form of PH with hydrocephalus,⁶ as well as a potential PH locus on chromosome 5p15 reflected by chromosome

rearrangements.⁷ Moreover, heterotopia with agenesis of the corpus callosum and ocular colobomas can be associated with a balanced translocation involving chromosomes 2p24 and 9q32.⁸ Finally, a recent report has documented a balanced reciprocal translocation t(1;6)(p12;p12.2) interrupting the mannosidase alpha, class 1A and glutathione S-transferase A2 genes, giving rise to PH.⁹

Previous studies have suggested a relationship between the connective tissue disorder Ehlers-Danlos

*These authors contributed equally to this work.

From the Division of Neurogenetics (Drs. Sheen, Hill, and Walsh, and R. Ravenscroft, V. Ganesh, A. Bodell, and K. Apse), Department of Neurology, Howard Hughes Medical Institute, Beth Israel Deaconess Medical Center, Boston; Montreal Neurological Institute and Hospital (Drs. Jansen, Dubeau, and Andermann), and the Department of Neurology and Neurosurgery, McGill University, Montreal, Quebec; Brigham and Women's Hospital (Dr. Chen), Cardiovascular Division, Boston; Epilepsy, Neurophysiology & Neurogenetics Unit (Drs. Parrini and Guerrini), Division of Child Neurology and Psychiatry, University of Pisa & IRCCS Fondazione Stella Maris, Pisa, Italy; Department of Paediatrics and Child Health (T. Morgan and Dr. Robertson), University of Otago, Dunedin, New Zealand; Departments of Hematology and Respiratory Medicine (Drs. Underwood and Wiley), Nepean Hospital, Sydney, Australia; Department of Neurology (Dr. Leventer), Royal Children's Hospital, & Murdoch Children's Research Institute, University of Melbourne, Victoria, Australia; Department of Radiology (Drs. Vaid, Ruiz, and Barkovich), University of California at San Francisco; Department of Pathology (Dr. Hutchins), The Johns Hopkins Hospital, Baltimore, MD; Department of Human Genetics (Drs. Menasha, Willner, and Geng), Mount Sinai Hospital, New York, NY; Division of Medical Genetics (Dr. Gripp and L. Nicholson), duPont Hospital for Children, Wilmington, DE; Department of Pediatrics (Dr. Berry-Kravis), Section of Neurology, Rush University Medical Center, Chicago, IL; Department of Human Genetics (Dr. Andermann), McGill University, Montreal, Quebec, Canada; Department of Epidemiology (Dr. Shugart), Johns Hopkins Bloomberg School of Public Health, Baltimore, MD; Service de Neurologie (Dr. Thomas), Hopital Pasteur, Nice, France; Ospedale Fatebenefratelli (Dr. Viri), Milan, Italy; Neuropsichiatria Infantile (Dr. Veggiotti), Istituto Mondino Pavia, Italy; and Program in Biological and Biomedical Sciences (Dr. Walsh), Harvard Medical School, Boston, MA.

Supported by Grant R-04–35 to R.G. from Fondazione Mariani and by grants to C.A.W. from the National Institute of Neurologic Disorders and Stroke (2R37 NS35129 and 1P01NS40043), the March of Dimes, and the McKnight Foundation. C.A.W. is an Investigator of the Howard Hughes Medical Institute. V.L.S. is supported by a grant from the NIMH (1K08MH/NS63886–01). V.L.S. is a Charles A. Dana fellow.

Received July 28, 2004. Accepted in final form October 4, 2004.

Address correspondence and reprint requests to Dr. C.A. Walsh, Harvard Medical School, Boston, MA 02115; e-mail: cwash@bidmc.harvard.edu

syndrome (EDS) and PH. Two single case reports described a variant of EDS, type unspecified, with PH.^{10,11} Both affected females exhibited focal seizures, irregular collagen fibrils, and aneurysms of the sinuses of Valsalva. Features including agenesis of the posterior corpus callosum, enlarged cisterna magna, panacinar emphysema, and myocardial infarction were also observed in either one but not both individuals.

Many of the same clinical and radiologic features seen in these two case reports can sometimes be seen in X-linked PH due to *FLNA* mutations. For example, most individuals with known *FLNA* mutations are female, present with seizures, and more variably, have vascular anomalies including aortic aneurysm, patent ductus arteriosus, and bicuspid aortic valve.^{1,12,13} Radiologic imaging demonstrates bilateral nodular heterotopia, which can be associated with thinning of the corpus callosum and an enlarged cisterna magna.¹⁴ In this study, we analyzed a number of patients with PH and features of EDS in order to determine their clinical features. Moreover, we examined whether affected individuals harbored mutations in the *FLNA* gene, performed a genomic screen on the X-chromosome for the single multiplex pedigree with PH and features of EDS, and addressed whether this pedigree had demonstrable loss of the *FLNA* protein expression or an intronic rearrangement of the *FLNA* gene.

Methods. The study includes two affected pedigrees (P1, P2), two previously reported sporadic cases (F3, F5),^{10,11} and seven additional affected individuals (F1, F2, F4, F6, F7, F8, M1). Patients undergoing genetic testing provided informed consent according to guidelines approved by the respective institutions' human subjects research review committees, and the Office of Human Research Protection. DNA was isolated from peripheral whole blood lymphocytes or from paraffin embedded sections using previously described protocols (Qiagen). Linkage analysis was performed on one pedigree (P1). Individuals studied by linkage analysis in Pedigree 1 include two affected individuals, an unaffected sibling, the parents, an affected aunt, and the obligate carrier grandmother. DNA sequence analysis was performed on affected individuals from this pedigree, the second pedigree (P2), as well as eight individuals with spontaneous presentations of PH and EDS features (F1, F2, F3, F4, F5, F7, F8, M1). Probands underwent MRI in a 0.5- or 1.5-Tesla scanner, using standard clinical imaging protocols.

Linkage analysis. A linkage screen at 10 cM of the X-chromosome was performed on the single pedigree (P1, family members II-2; III-4, 5, 6; and IV-3, 4, 5). PCR was performed using the 10 cM ABI linkage mapping set for the X-chromosome: *DXS1227*, *DXS990*, *DXS986*, *DXS987*, *DXS993*, *DXS1073*, *DXS8091*, *DXS1106*, *DXS1047*, *DXS1001*; *DXS1001*, *DXS1068*, *DXS1214*, *DXS8055*, *DXS8051*, *DXS8043*, *DXS1060*, *DXS 1226*, *DXS 991*. Additionally, primers adjacent to the *FLNA* locus were used to evaluate potential linkage (*DXS1200*, *DXS998*, *DXS1193*, and *DXS8069*). Samples were analyzed on an ABI Prism 3100 genetic analyzer and alleles were determined using a standard software package (Genotyper Analysis). Two-point lod scores were calculated using the MLINK statistical program.¹⁵ For linkage analysis, the disorder was assumed to be X-linked with varying penetrance from 60 to 99% in males and females. In this family, we assumed a disease allele frequency of 1 in 10,000 and 8 alleles per marker at an equal allele frequency (12.5%).

Sequencing. PCR amplification was performed on genomic DNA from affected individuals (P1/IV-4, P1/IV-5, P2/II-4, F1, F2, F3, F4, F5, F7, F8, M1) using previously published primers for sequencing *FLNA*.¹² Greater than 95% of the *FLNA* exons were sequenced in each individual except F3 in which the poor quality of the DNA from the paraffin sections only allowed analysis of

about 50% of the exons. Sequencing was also not performed on individual F6 for whom genomic DNA was not available. The amplification products were purified (PSI/Clone PCR 96, Adelphia, NJ) and sequenced by the Dana-Farber/Harvard Cancer Center (DF/HCC) High-Throughput DNA Sequencing Facility using standard techniques. The sequenced exon and intron/exon boundaries were compared against consensus sequences obtained from the National Center for Biotechnology Information (NCBI, reference #NT 025965) Database using standard software for DNA sequencing analysis (Sequencher, version 3.1.1).

Single stranded conformational polymorphism (SSCP) analyses. SSCP analysis was performed following slight modifications of previously published methods.¹² Screening was performed on F5, M1.

Western blot analyses. Methods followed slight differences from previously published protocols.⁵ In brief, EBV-transformed lymphoblasts from patients with known *FLNA* mutations, PH without *FLNA* mutations, and PH with EDS (P1, IV-5) were harvested, solubilized in lysis buffer, separated on a 7.5% SDS-PAGE gel, and transferred onto PVDF membrane. Membranes were probed with anti-filamin A antibody (Novacastra) and binding was detected by enhanced chemiluminescence.

Southern blot analyses. Southern blotting was performed following previously published methods.¹⁶ Genomic DNA samples were prepared from whole blood or EBV-transformed lymphoblasts (Qiagen). DNA samples (10 µg) were digested with EcoRI, electrophoresed on a 0.6% agarose gel for 24 hours at 45V and transferred to Hybond N+ membranes (Amersham), hybridized with 32P dCTP randomly labeled probe (Megaprime DNA labeling kit, Amersham), and washed. Probe A corresponds to the 5' end of *FLNA* and was generated by PCR using the primer pair (TCCAG-CAGAACACTTTTCACG, GTCCCAAGAGTCCCAGTCAG) with the *FLNA* cDNA as a template. Probe B corresponds to the 3' end of *FLNA* and was generated by the primer pair (GTCTGCTTACG-GAGCAGGTC, TGTACTCCCCCTGTCTCTG) with the *FLNA* cDNA as a template.

Results. *Ehlers-Danlos variant form of PH.* The diagnosis of PH was based on radiographic findings and the diagnosis of EDS was based on the clinical history consistent with the suggested diagnostic criteria¹⁷ (table).

Pedigree 1. See figure 1A. An affected 7-year-old girl (IV-5) presented with a single seizure and tic disorder at age 6. She otherwise achieved appropriate developmental milestones and grade level performance. On examination, her head circumference was 53.7 cm (97th percentile). Her skin had normal texture, turgor, and elasticity. The joints showed ligamentous laxity with hyperextension of the knees and curvature of the lower extremities (genu recurvatum). MRI of the brain demonstrated bilateral periventricular nodular heterotopia with greater involvement of the right as compared to the left trigone. Similarly, increased PH was noted in the left vs the right frontal ventricular zone. Nodules ranged from less than 0.5 cm to greater than 1 cm in diameter (figure 2, A and B).

An affected 9-year-old girl (IV-4) was evaluated because of the presentation of her sibling. Her perinatal course was complicated by pneumonia and bilateral hearing loss from chronic ear infections. She has a history of migraines, but no seizures. She achieved appropriate developmental milestones. Her skin had normal texture, turgor, and elasticity. The joints showed ligamentous laxity with genu recurvatum of the knees. MRI of the brain demonstrated nodular heterotopia, scattered along the superolateral aspects of the lateral ventricles. Involvement was greater in the left than right lateral ventricle.

The mother of the two children (III-5) has no notable past medical history aside from migraines. She has had two miscarriages. She works as a teacher. She declined MRI of the brain.

The affected 24-year-old maternal aunt (III-6) has a

Table Clinical and radiologic features of patients with periventricular heterotopia in Ehlers-Danlos syndrome

Family/patient	Age, y/sex	Radiographic findings	Seizures/cognitive delay	Skin manifestations	Pulmonary/vascular anomalies	Filamin A mutations
P1						
IV-4	7/F	PH	Seizures	JH	None	None
IV-5	9/F	PH	None	JH	None	
P2						
II-3	54/F	PH	Seizures	JH	None	None
III-1	25/F	PH	Seizures	JH	Pulmonary hemorrhage	
F1	29/F	PH	Seizures/mild delay	JH	AA	None
F2	16/F	PH	None	JH	AA	4147delG (exon 25)
F3 ²²	30/F	PH	None	JH	AA	None
					Panacinar emphysema	
					Myocardial infarct	
F4	18/F	PH	Seizures/mild delay	JH	None	None
F5 ¹⁰	24/F	PH	Seizures	JH	AA	None
F6	40/F	PH	None	None	AA	Not tested
					Bullous emphysema	
					Hemoptysis	
F7	13/F	PH	None	JH	Mitral and aortic valves with myxomatous changes, mild reflux	2762delG (exon 19)
F8	15/F	PH	Seizures/mild delay	JH	AA	C116G (exon 2) → A39G
M1	1/M	PH	Moderate delay	JH	None	None

PH = periventricular heterotopia; JH = joint hypermobility; AA = aortic aneurysm.

seizure disorder first diagnosed at age 22 years. She has a history of migraines with chronic daily headaches. Her joints showed increased flexibility, and her skin was very soft with easy tendency to bruise. She has a prolapsed atrial valve, and poor circulation with spider veins. She

describes difficulty with reading and spelling. MRI of the brain (not shown) demonstrated bilateral large (1 cm), near-contiguous nodular heterotopia along the lateral ventricles.

The 60-year-old maternal grandmother (II-2) has had two miscarriages and a stillborn son. She has had no history of seizures or seizure-like episodes and no complaint of headaches. She has smooth, stretchy skin with very flexible joints. She has not undergone neuroimaging.

The maternal grandmother's sister (II-3) and the sister's daughter (III-10) are presumably affected. Although no formal radiologic imaging was available for review, both women had seizures, dyslexia, and hyperflexible joints.

Pedigree 2. See figure 1B. An affected 25-year-old woman (III-1) initially presented with catamenial seizures at age 17 years. She subsequently developed recurrent episodes of pulmonary hemorrhage in association with the seizure events. She has a history of multiple recurrent patellar dislocations, requiring surgery. On examination, she had short stature with kyphoscoliosis. Her teeth were irregular and she had multiple facial dysmorphism including hypertelorism, a depressed nasal bridge, and cupid bow mouth. Her neck was short and webbed, her hands and feet were hypoplastic with small nails, and her joints were hypermobile. Her skin was soft and easily bruised, and she had papyraceous scars on the right knee. On neuropsychological testing, she had below average cognitive performance with weakness on memory recall and poor drawing capabilities. MRI showed bilateral cerebral heterotopia, and partial agenesis of the corpus callosum. EEG showed excessive slow wave activity. Her testing was also notable for mild thrombocytopenia (platelet count of 88 K/mm³) and splenomegaly by ultrasound. CT of the abdo-

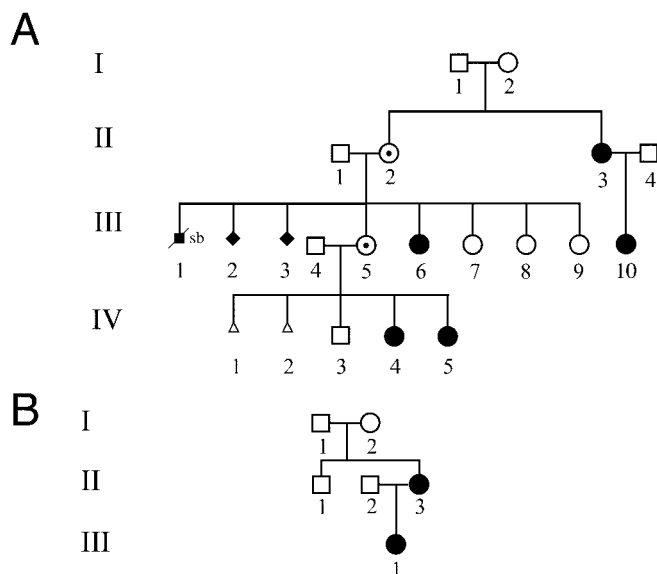


Figure 1. Familial periventricular heterotopia and Ehlers-Danlos syndrome (PH and EDS). (A) Schematic of Pedigree 1 (P1). (B) Schematic of Pedigree 2 (P2). Black circles = affected individuals with EDS features and known or presumed periventricular heterotopia (PH). Black diamonds = spontaneous abortions. White circles with black dots = obligate carriers. Small black square = stillborn male.

men was otherwise unremarkable. Echocardiogram demonstrated no aortic root dilatation; there was mild aortic and tricuspid regurgitation. Evidence of old and new hemorrhage was confirmed on pulmonary lavage and biopsy. Lung biopsy showed no evidence of vasculitis or inflammation. Antibodies to glomerular basement membrane and neutrophil cytoplasm proteins were not detected and immunofluorescence staining for IgG, IgA, IgM, C3, C1q, fibrinogen, and transferrin was unremarkable.

The affected 53-year-old mother (II-3) has had epilepsy since childhood. She was also documented to have mild thrombocytopenia (platelet count of 68 K/mm³). By report, radiologic imaging of the brain also documented PH.

Sporadic cases. Female 1. The affected 29-year-old woman developed seizures at age 14 years, thought to be secondary to a left-sided brain hemangioma. She had a prior history of psychotic hallucinations and violent behavior. On examination, she had no documented neurologic deficits. Her skin was velvety with normal recoil and stretch. The digits were hyperextensible. She had scoliosis, pectus excavatum, and a repaired cleft lip and palate. MRI of the brain was notable for diffuse, symmetric nodular gray matter heterotopia lining the lateral ventricles (figure 2C). Echocardiogram revealed a non-coronary sinus of Valsalva aneurysm with severe aortic regurgitation.

Female 2. The affected 16-year-old girl was previously diagnosed with classic EDS in the first year of life due to hypotonia, joint laxity, and hyperextensible skin. She has a history of easy joint dislocation including the knees and subluxation of the thumbs and clavicles. On examination, she had no focal neurologic findings. Her height fell in the 75th percentile with arm span 8 cm less than the height. She had hyperextensible chest skin and flat feet. MRI of the brain was notable for right bilateral nodular heterotopic gray matter, which was greater than on the left, a small arachnoid cyst in the left sylvian fissure, and an enlarged cisterna magna. Nodules appeared clustered, irregular in their conformation, and non-contiguous (figure 2, D through F). MRI/MRA of the intracranial, thoracic, abdominal, and pelvic vessels demonstrated marked dilatation of the ascending aorta and duplex right kidney.

Female 3. This affected 30-year-old woman has previously been described.¹¹ She had generalized tonic clonic seizures that began at age 21 years. There was no mention of an abnormal neurologic examination. She had hypotonia, and hypermobility of the joints with frequent, spontaneous dislocations. Her skin was velvety and somewhat hyperextensible. She developed progressive dyspnea and chest pain, resulting in congestive heart failure and transient ectopy. She died of refractory ventricular fibrillation. Autopsy of the brain revealed bilateral periventricular nodular heterotopia and capillary vascular malformations similar to those described in a PH case with a confirmed *FLNA* mutation.¹⁸ The heart was enlarged and had aneurysms of both noncoronary and left coronary sinuses of Valsalva. Marked panacinar emphysema were seen in the lungs. Electron microscopic examination of the skin revealed an irregular size and shape of the collagen fibrils.

Female 4. The affected 18-year-old woman developed poorly controlled complex partial seizures at age 4 years. On examination, she had a full scale IQ of 67, a left homonymous hemianopia with strabismus, and mild left hemiparesis. She had asymmetric facies, hypotelorism,

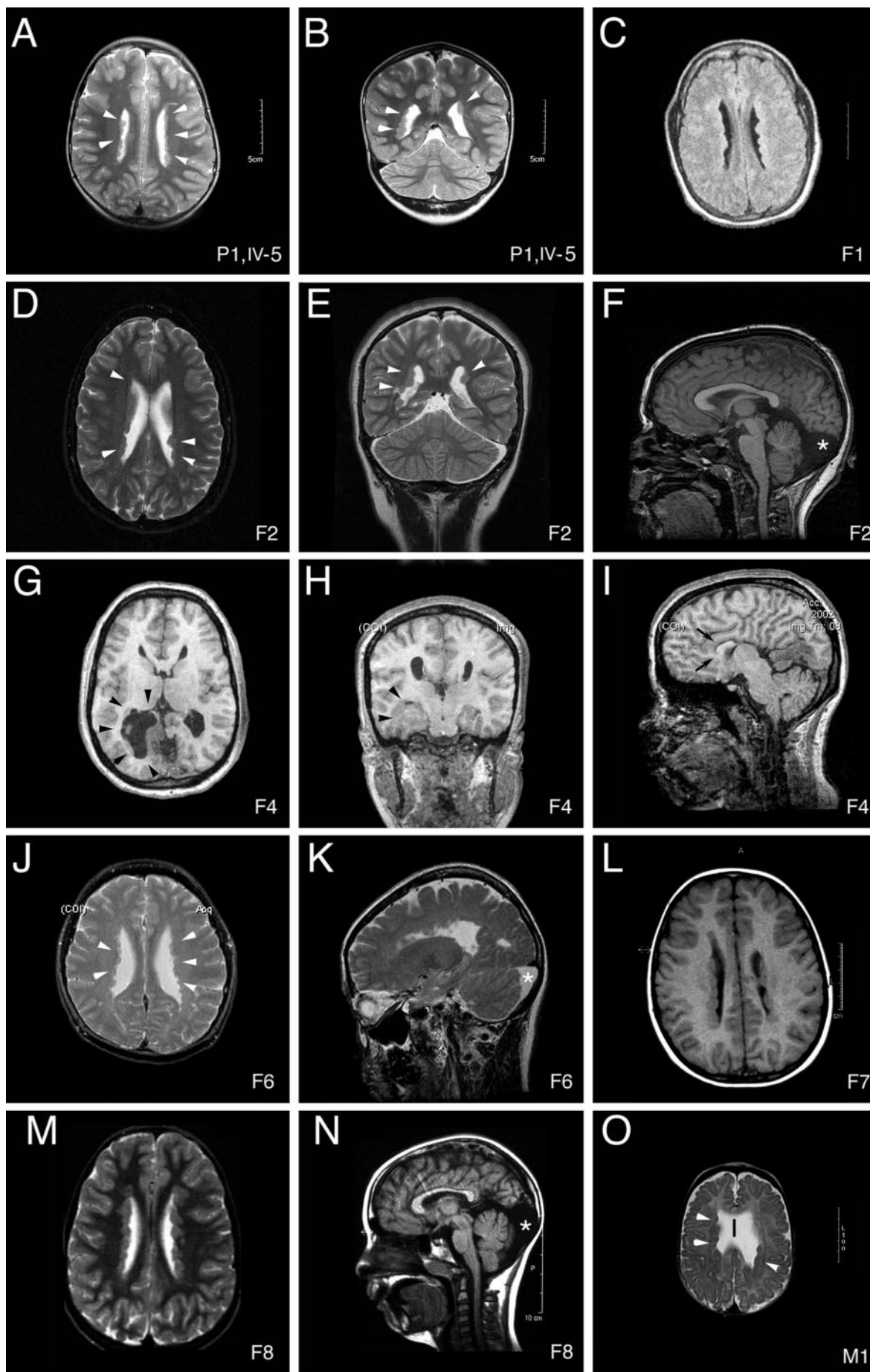
hypermobility of the joints, and marked elasticity of the skin. EEG showed multifocal sharp and spike waves. MRI of the brain revealed partial agenesis of the corpus callosum with preservation of 1 cm of the genu. The cingulate gyrus was poorly formed and the ventricles were enlarged, particularly involving the occipital horn of the lateral ventricle. A large subcortical heterotopia extended from the medial surface of the right occipital lobe to the tip of the temporal lobe, involving the hippocampus and amygdala and protruding into the right ventricle. The overlying cortex exhibited an abnormal gyral pattern in the right posterior quadrant. Periventricular heterotopia were seen in the posterior walls of the lateral ventricles bilaterally (figure 2, G through I).

Female 5. The affected 24-year-old woman has previously been described.¹⁰ She developed complex partial seizures at age 14 years. On examination, she had an IQ of 110 with no focal neurologic findings. She had hyperextensibility of the small joints, smooth velvety skin, hyperextensible skin, and atrophic scars at sites of previous laceration. She also had scoliosis and parrot-like facies. EEG showed isolated spike waves localized over the left frontocentral area of left hemispheric sharp-wave discharges. MRI of the brain showed bilateral periventricular nodular heterotopia, agenesis of the posterior portion of the corpus callosum, and an enlarged cisterna magna. Skin biopsy showed irregular and frayed collagen fibers. MRI of the heart demonstrated dilatation of the noncoronary sinuses of Valsalva.

Female 6. The affected 40-year-old woman presented with transient right-sided monocular blindness at age 39 years. She had previously undergone aortic root replacement for aortic dilatation and repair of her aortic valve for insufficiency. She had presented with hemoptysis and was diagnosed with bullous emphysema. There is no history of seizures. Neurologic examination was normal. She had no clear skin manifestations but a complaint of arthritis. MRI of the brain demonstrated bilateral nodular heterotopia with mega cisterna magna. Nodules were generally discrete, contiguous, and small (<0.5 cm) in diameter (figure 2, J and K). Pulmonary function tests revealed a severe obstructive ventilatory defect.

Female 7. The affected 13-year-old girl presented with developmental delay, sitting at 8 months, and walking at 27 months of age. She was cognitively normal and progressed normally through school. She has not developed seizures. She was clinically diagnosed with classic EDS at age 3 years, which was confirmed by biochemistry (abnormal collagen V/I ratio in cutaneous fibroblasts; value = 0.10 vs normal = 0.15 to 0.22). At age 5 years, the patient started experiencing headache, which has worsened. Clinical examination was consistent with typical features of EDS, including joint hypermobility. She had no dysmorphic features. Echocardiogram of the heart revealed myxomatous borders along the mitral and aortic valves and mild reflux. MRI of the brain showed characteristic bilateral periventricular heterotopia (figure 2L).

Female 8. The affected 15-year-old girl has a history of focal seizures. On examination, she had borderline cognitive level (full-scale IQ = 78) and psychotic behavior. She had a high arched palate with mandibular hypoplasia. Truncal examination was notable for scoliosis and pectus excavatum (foveated/funnel chest). She had hypermobility



of the joints, predominantly affecting the distal joints. She was diagnosed with an aneurysm of the sinus of Valsalva with hyperelasticity of the large vessels. Molecular study of the fibrillin 1G for Marfan syndrome was negative. MRI of the brain showed bilateral periventricular nodular heterotopia and a mega cisterna magna (figure 2, M and N).

Male 1. The affected 20-month-old boy presented with perinatal gastroschisis and bilateral lateral ventricular enlargement with absent septum pellucidum by ultrasound. He has had no seizures to date. On examination, he had dysconjugate gaze and a right-sided strabismus, right optic nerve hypoplasia, and bilateral conductive hearing loss. He reached for objects and tracked appropriately. He was able to stand with minimal help, scoot, and roll over. He did not start crawling until 20 months of age. He had hyperextensibility of the fingers, rubbery and loose skin, and webbing between his digits. MRI of the brain demonstrated bilateral, noncontiguous nodular heterotopia, absent septum pellucidum, and mild ventriculomegaly. Heterotopia were more apparent along the posterior walls of the lateral ventricles. Involvement was also greater on the right as opposed to the left ventricular lining (figure 2O). MRI of the mother was normal.

Genetic analysis of *FLNA*. Given the female predominance in the Ehlers-Danlos variant of PH (13 of 14 affected individuals), the apparently more severe phenotype in the one male studied, and the shared similarities with X-linked PH due to *FLNA* mutations, we sought to evaluate whether the connective tissue abnormalities seen in these individuals represented a variant presentation of PH due to *FLNA* mutations. Genomic sequencing of greater than 95% of the 48 *FLNA* exons identified a 4147delG single base pair deletion (exon 25) in individual F2, resulting in a frameshift and presumed truncation mutation (figure 3A). The deletion also results in the demonstrable loss of an AluI restriction enzyme cut site. A second mutation 2762del G single base pair deletion (exon 19) was found in individual F7, resulting in a frameshift and presumed truncation mutation. This mutation was not present in 167 control chromosomes. A third mutation was identified in individual F8, who harbored a 116C > G (exon 2) single point mutation, resulting in an A39G change. This mutation was not present in the mother or 236 control chromo-

somes. Due to the quality of genomic DNA, only 50% of the *FLNA* sequence was excluded for mutations in individual F3. Sequencing was not performed in individual F6, for whom genomic DNA was not available.

As the absence of exonic mutations did not exclude intragenic or noncoding mutations in *FLNA*, we performed linkage analysis on the X-chromosome of one affected pedigree (P1). The second pedigree (P2) did not have a sufficient number of individuals in order for informative linkage. Two-point analyses on P1 excluded the entire X-chromosome except for Xq28, with a lod score of < -2.0 over most of the chromosome. In contrast, linkage could not be excluded from Xq28, which gave a moderately positive lod score of 1.19 (the theoretical maximal positive score for a pedigree of this size is 1.19) (figure 3B). Given the strong evidence for X-linkage of the trait, both in this pedigree as well as from the female-male bias in our sporadic cases, these linkage results are most consistent with linkage overlapping the *FLNA* gene in Xq28, though they are not definitive.

We therefore examined the *FLNA* protein expression of transformed lymphoblasts from an affected female individual (P1/IV-5) of this pedigree. Western blotting showed absence of *FLNA* protein in the PH EDS sample (figure 3C). Finally, the *FLNA* locus is a common region of inversion mediated by inverted repeats,¹⁶ raising the possibility of inappropriate DNA rearrangement and formation of a fusion or truncated protein. Since this rearrangement would not necessarily be apparent on exonic *FLNA* sequencing, we performed Southern blotting on genomic DNA from multiple individuals of the P1 pedigree. Probes designed against the middle and 3' end of the *FLNA* genomic region, however, failed to identify any abnormally sized bands (figure 3D). Additionally, we examined the noncoding regions of *FLNA* using GeneScan, Assembly, and human EST/mRNA databases; these databases did not demonstrate any nested genes within the noncoding regions of *FLNA*, which might be responsible for the EDS features.

Discussion. We examine the clinical and potential genetic overlap between PH with EDS and X-linked dominant PH due to *FLNA* mutations. The female

Figure 2. Brain MRI appearance of affected individuals with the Ehlers-Danlos variant of periventricular heterotopia (PH). (A) Axial T2-weighted image of patient P1 (IV-5) demonstrates bilateral gray matter nodules, lining the lateral ventricles with left > right predominance in the frontal cortex (white arrowheads). (B) Coronal T2-weighted image of the same patient shows a right > left predominance of gray matter nodules in the trigone (white arrowheads). (C) Axial T1-weighted image of patient F1 demonstrates characteristic bilateral PH. (D, E) Axial and coronal T2-weighted images of patient F2 reveal PH that is asymmetric, noncontiguous, and irregular in shape (white arrowheads). (F) Sagittal T1-weighted image of the same patient shows a mega cisterna magna (asterisk). (G, H, I) Axial, coronal, and sagittal T1-weighted images of patient F4 revealed PH along the posterior walls of the lateral ventricles bilaterally with a large subcortical heterotopia extending from the medial surface of the right occipital lobe to the tip of the temporal lobe (black arrowheads in G, H). Abnormal gyral patterning in the occipital cortex extended over the enlarged occipital horn of the right lateral ventricle. Partial agenesis of the corpus callosum (black arrows in I) and a poorly formed cingulate gyrus were also observed. (J, K) Axial and sagittal T2-weighted image of patient F6 demonstrated bilateral nodular heterotopia (white arrowheads) with mega cisterna magna (asterisk). (L) Axial T1-weighted image of patient F7 demonstrates characteristic bilateral PH. (M, N) Axial T2-weighted and sagittal T1-weighted images of patient F8 demonstrate the same bilateral PH and an enlarged cisterna magna (asterisk). (O) Axial T2-weighted image of patient M1 was notable for bilateral gray matter along the ventricles (white arrowheads), absent septum pellucidum (black line), and mild ventriculomegaly.

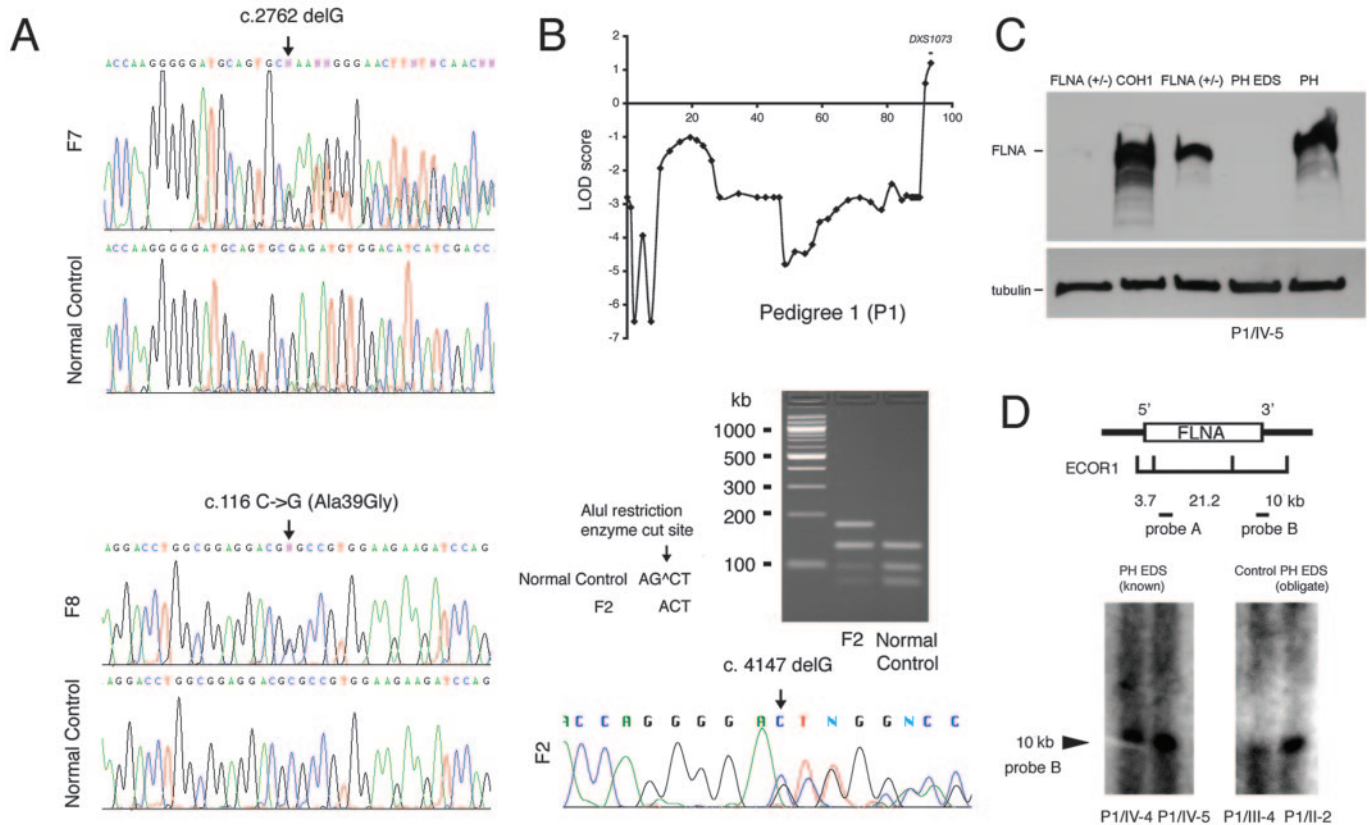


Figure 3. Some cases of PH with EDS are due to disruption in *FLNA*. (A) In affected individual F7, 2762delG results in a predicted premature protein truncation. In affected individual F8, 116C->G predicts the amino acid substitution A39G. In affected individual F2, 4147delG results in a predicted premature protein truncation. This deletion results in the loss of an *AluI* restriction enzyme cut site on one allele. (B) In Pedigree 1, two-point lod score analyses excluded the entire X-chromosome except for Xq28 (marker DXS1073), which coincides with the *FLNA* locus. Linkage could not be excluded for Xq28, which gave a moderately positive lod score of 1.19 (the maximal theoretical lod score for this pedigree). (C) Western blot demonstrates absence or reduction of the *FLNA* protein in individuals known to have heterozygous *FLNA* mutation (*FLNA* ±) in this X-linked dominant disorder and in the individual with PHD EDS (IV-5) from Pedigree 1. There is normal *FLNA* expression in a Cohen syndrome patient carrying a *COH1* gene mutation, and an individual with PH, no EDS, and no documented *FLNA* mutation. (D) Southern blot with probe B demonstrates the presence of an appropriately sized 10 kb band corresponding to the 3'-end of the *FLNA* genomic region after *ECOR1* digestion of DNA from multiple affected or unaffected individuals in P1. Similar results were obtained with probe A corresponding to the 5' end of the *FLNA* genomic region (data not shown).

predominance of affected individuals (both pedigrees have only affected females and 8 of 9 sporadic cases of PH and EDS are female) suggests an X-linked dominant disorder. Apart from the joint and skin anomalies, PH with EDS shares identical features seen in X-linked dominant PH due to *FLNA* mutations, including the radiologic hallmark of bilateral periventricular heterotopia with often associated findings of an enlarged cisterna magna and thinning or agenesis of the corpus callosum. Clinically, seizures and aortic aneurysms are also seen in both disorders. Furthermore, *FLNA* can clearly contribute to EDS features, as three of the affected females with PH and EDS had an exonic mutation. The absence of an exonic *FLNA* mutation in the remaining cases also does not exclude *FLNA* as a causal gene. Intragenic mutations can similarly contribute to the PH and EDS phenotype; this possibility is supported

by the absence of detectable *FLNA* protein in Pedigree 1, which did not harbor a demonstrable mutation in the coding region. However, it suggests that *FLNA* mutations, if they cause PH with EDS, do so by alterations that change *FLNA* expression levels. Finally, in addition to *FLNA*, other as yet unidentified genes could potentially cause PH and EDS.

Patients with PH and EDS collectively do not fall into any particular EDS classification. The risk of arterial rupture from aortic root dilatation and premature death raises some similarities to the vascular form of EDS.¹⁹ The prevalent findings of joint hypermobility with the tendency for recurrent dislocations are more suggestive of the hypermobility type of EDS or the familial forms of joint laxity.^{20,21} Alternatively, the skin hyperelasticity, increased tendency to bruise, and abnormal scarring are consistent with classic EDS.²² The predominance of af-

ected females in this disorder suggests an X-linked inheritance pattern, although the clinical characteristics or mode of inheritance are distinct from the X-linked occipital horn syndrome (EDS type IX).¹⁷ While PH with EDS shares some similarities with various EDS types, the associated CNS findings of heterotopia suggest that this is a distinct syndrome.

EDS in PH represents a rare variant of a relatively uncommon disorder. In the current study, 8 of 94 sporadic female PH cases (8.5%) were identified to share EDS features, and 3 of these 8 cases (38%) have detectable *FLNA* mutations. Prior studies have also suggested that 19% of sporadic female PH cases carry an identifiable exonic *FLNA* mutation.¹⁷ Based on this ascertainment, the frequency of EDS in PH with known *FLNA* mutations would approximate 17%. Thus, there is a twofold greater likelihood that an individual with PH and EDS features carries a *FLNA* mutation compared to the population with PH and EDS in general.

Mutations within *FLNA* can give rise to a wide variety of clinical syndromes, consistent with the diverse functions implicated with this gene.^{1,3,13,23} Generally loss-of-function mutations have been thought to cause periventricular heterotopia within the brain and can be associated with cardiac and blood abnormalities.¹² The current study also suggests that EDS features may also be associated with loss of *FLNA* function as two truncation mutations in this gene (both in the IgG-like repeats) were identified in individuals F2 and F7. Additionally, specific mutations within the actin-binding region or rod domain repeats likely lead to gain-of-function mutations, resulting in four X-linked human disorders: otopalatodigital syndrome types 1 and 2, frontotaphyseal dysplasia (FMD), and Melnick-Needles syndrome. An individual with both PH and FMD has been described to carry two aberrant transcripts near the carboxyl terminus of *FLNA*, suggesting some potential overlap in these disorders.²⁴ PH with EDS may similarly comprise an overlapping syndrome; one female (F8) carries a mutation in the actin-binding domain, giving rise to a high arched palate and aneurysm of the sinus of Valsalva with hyperelasticity of the large vessels (as seen in a variant form of FMD²⁵), and periventricular heterotopia (consistent with X-linked PH). Finally, the failure to detect an exonic mutation in many of the PH with EDS patients raises the possibility that the EDS features in this syndrome may result from other specific rearrangements or mutations within the *FLNA* intronic, promoter, or untranslated regions.

The exact relationship between the disrupted neuronal migration present in PH and the defects in connective tissue seen in EDS are not yet apparent. Disruption in cell adhesion, however, may provide a common mechanism, giving rise to both features. In general, the various types of EDS are caused by defects in collagen or the processing and release of collagen, thereby altering the cross-linkage and adhesion of collagen fibrils in the extracellular matrix.

Similarly, the two known causes of PH may also be involved in cell adhesion. In X-linked PH, *FLNA* mediates the association of migfilin with the actin cytoskeleton, and Mig-2 (mitogen inducible gene-2) recruits migfilin to the cell-matrix adhesions.²⁶ The β -integrins which are involved in cell-extracellular matrix and cell-cell interactions have also been shown to bind filamin and mediate cell adhesion and migration.²⁷ In PH with microcephaly, mutations of *ARFGEF2* impair vesicular trafficking of certain adhesion molecules such as E-cadherin and β -catenin from the Golgi apparatus to the cell surface.⁵ In this context, impaired cellular adhesion may be responsible for both the loss in connective tissue strength and elasticity in EDS and prevent post-mitotic neurons from migrating from the ventricular zone into the cortex in PH. However, this potential mechanism requires further investigation and remains to be shown.

The current report extends upon the known phenotype of X-linked dominant PH due to *FLNA* mutations, and suggests that EDS features can be associated with this disorder. Moreover, multiple members of the filamin family of actin-binding proteins likely contribute to this phenotype, as mutations in filamin B are associated with joint laxity and dislocations.²⁸ Most affected individuals with PH and EDS do not appear to have an exonic *FLNA* mutation although they share the same clinical and radiologic characteristics of X-linked PH; this raises the possibility that the EDS features of this syndrome may result from unique noncoding alleles of *FLNA*. Finally, whether cell adhesion represents a common molecular pathway that gives rise to both PH and EDS remains to be determined.

Acknowledgment

The authors thank Dr. Andrew Kornberg for assistance in patient recruitment.

References

1. Fox JW, Lamperti ED, Eksioğlu YZ, et al. Mutations in filamin 1 prevent migration of cerebral cortical neurons in human periventricular heterotopia. *Neuron* 1998;21:1315–1325.
2. Dobyns WB, Guerrini R, Czapansky-Beilman DK, et al. Bilateral periventricular nodular heterotopia with mental retardation and syndactyly in boys: a new X-linked mental retardation syndrome. *Neurology* 1997;49:1042–1047.
3. Guerrini R, Mei D, Sisodiya S, et al. Germline and mosaic mutations of *FLN1* in men with periventricular heterotopia. *Neurology* 2004;63:51–56.
4. Sheen VL, Topcu M, Berkovic S, et al. Autosomal recessive form of periventricular heterotopia. *Neurology* 2003;60:1108–1112.
5. Sheen VL, Ganesh VS, Topcu M, et al. Mutations in *ARFGEF2* implicate vesicle trafficking in neural progenitor proliferation and migration in the human cerebral cortex. *Nat Genet* 2004;36:69–76.
6. Sheen VL, Basel-Vanagaite L, Goodman JR, et al. Etiological heterogeneity of familial periventricular heterotopia and hydrocephalus. *Brain Dev* 2004;26:326–334.
7. Sheen VL, Wheless JW, Bodell A, et al. Periventricular heterotopia associated with chromosome 5p anomalies. *Neurology* 2003;60:1033–1036.
8. Ramocki MB, Dowling J, Grinberg I, et al. Reciprocal fusion transcripts of two novel Zn-finger genes in a female with absence of the corpus callosum, ocular colobomas and a balanced translocation between chromosomes 2p24 and 9q32. *Eur J Hum Genet* 2003;11:527–534.
9. Leeftang EP, Marsh SE, Parrini E, et al. A patient with bilateral periventricular nodular heterotopia and polymicrogyria with an apparently balanced reciprocal translocation t(1;6)(p12;p12.2) interrupting the mannosidase alpha, class 1A, (*MAN1A2*) and glutathione S-transferase A2 (*GSTA2*) genes. *J Med Genet* 2003.

10. Thomas P, Bossan A, Lacour JP, et al. Ehlers-Danlos syndrome with subependymal periventricular heterotopias. *Neurology* 1996;46:1165–1167.
11. Cupo LN, Pyeritz RE, Olson JL, et al. Ehlers-Danlos syndrome with abnormal collagen fibrils, sinus of Valsalva aneurysms, myocardial infarction, panacinar emphysema and cerebral heterotopias. *Am J Med* 1981;71:1051–1058.
12. Sheen VL, Dixon PH, Fox JW, et al. Mutations in the X-linked filamin 1 gene cause periventricular nodular heterotopia in males as well as in females. *Hum Mol Genet* 2001;10:1775–1783.
13. Moro F, Carrozzo R, Veggiotti P, et al. Familial periventricular heterotopia: missense and distal truncating mutations of the FLN1 gene. *Neurology* 2002;58:916–921.
14. Poussaint TY, Fox JW, Dobyns WB, et al. Periventricular nodular heterotopia in patients with filamin-1 gene mutations: neuroimaging findings. *Pediatr Radiol* 2000;30:748–755.
15. Terwilliger JD OJ. *Handbook of human genetic linkage*. Baltimore: The Johns Hopkins University Press, 1994.
16. Small K, Iber J, Warren ST. Emerin deletion reveals a common X-chromosome inversion mediated by inverted repeats. *Nat Genet* 1997;16:96–99.
17. Beighton P, De Paepe A, Steinmann B, Tsipouras P, Wenstrup R.J. Ehlers-Danlos syndromes: revised nosology, Villefranche, 1997. Ehlers-Danlos National Foundation (USA) and Ehlers-Danlos Support Group (UK). *Am J Med Genet* 1998;77:31–37.
18. Kakita A, Hayashi S, Moro F, et al. Bilateral periventricular nodular heterotopia due to filamin 1 gene mutation: widespread glomeruloid microvascular anomaly and dysplastic cytoarchitecture in the cerebral cortex. *Acta Neuropathol (Berl)* 2002;104:649–657.
19. Germain DP, Herrera-Guzman Y. Vascular Ehlers-Danlos syndrome. *Ann Genet* 2004;47:1–9.
20. Nuytinck L, Freund M, Lagae L, et al. Classical Ehlers-Danlos syndrome caused by a mutation in type I collagen. *Am J Hum Genet* 2000;66:1398–1402.
21. Beighton P, de Paepe A, Danks D, et al. *International Nosology of Heritable Disorders of Connective Tissue*, Berlin, 1986. *Am J Med Genet* 1988;29:581–594.
22. Eisenbeiss C, Martinez A, Hagedorn-Greiwe M, et al. Reduced skin thickness: a new minor diagnostic criterion for the classical and hypermobility types of Ehlers-Danlos syndrome. *Br J Dermatol* 2003;149:850–852.
23. Robertson SP, Twigg SR, Sutherland-Smith AJ, et al. Localized mutations in the gene encoding the cytoskeletal protein filamin A cause diverse malformations in humans. *Nat Genet* 2003;33:487–491.
24. Zenker M, Rauch A, Winterpacht A, et al. A dual phenotype of periventricular nodular heterotopia and frontometaphyseal dysplasia in one patient caused by a single FLNA mutation leading to two functionally different aberrant transcripts. *Am J Hum Genet* 2004;74:731–737.
25. Takahashi K, Kuwahara T, Tanigawara T, et al. Frontometaphyseal dysplasia: patient with ruptured aneurysm of the aortic sinus of Valsalva and cerebral aneurysms. *Am J Med Genet* 2002;108:249–251.
26. Tu Y, Wu S, Shi X, Chen K, Wu C. Migfilin and Mig-2 link focal adhesions to filamin and the actin cytoskeleton and function in cell shape modulation. *Cell* 2003;113:37–47.
27. Calderwood DA, Huttenlocher A, Kiosses WB, et al. Increased filamin binding to beta-integrin cytoplasmic domains inhibits cell migration. *Nat Cell Biol* 2001;3:1060–1068.
28. Krakow D, Robertson SP, King LM, et al. Mutations in the gene encoding filamin B disrupt vertebral segmentation, joint formation and skeletogenesis. *Nat Genet* 2004;36:405–410.